Available online at www.sciencedirect.com
ScienceDirect
Journal of Sound and Vibration 306 (2007) 215–226
JOURNAL OF SOUND AND VIBRATION
www.elsevier.com/locate/jsvi

Analysis of source models for two-dimensional acoustic systems using the transfer matrix method

Zhaoyu Huang*, Weikang Jiang

State Key Lab of Mechanical System & Vibration, Institute of Vibration, Shock & Noise, Shanghai Jiaotong University, Shanghai 200240, China

Received 1 June 2006; received in revised form 9 April 2007; accepted 13 May 2007
Available online 19 June 2007

Abstract

The point sound source model calculating the transfer matrix of thin acoustic cavities has been extensively utilized in analyzing certain mufflers. However, the computational result of the transfer matrix is not valid due to the singularity of the point source model. In this paper, a surface source model for thin acoustic cavities is discussed for its convergence characteristic and pressure responses on the source surface, which shows that the pressure responses on the surface are not uniform and the computational results of the transfer matrix coefficient are questionable. Finally, the circular line sound source model is suggested. Through theoretical analysis and computational examples, it is shown that this model avoids the singularity of source and obtains the uniform pressure responses on the circular line. Compared to the circular surface source, it is more convenient and has approximate averaged pressure responses if the circular radius is reasonably selected.

1. Introduction

The thin cavity system is extensively used as the model of certain mufflers in small sealed refrigeration compressors and the automotive industry. Such mufflers can be fitted into the small spaces and narrow gaps between the rotor, motor and shell [1]. The transfer matrix method is a very convenient way to analyze some complicated acoustic systems, where transfer matrices between the input and output variables of an acoustic cavity can be obtained in the frequency domain.

One-dimensional or lumped parameter method is available for many applications [2,3]. However, the lumped parameter analysis is only suitable for some specific cases in which the cross-section dimensions of typical components are small enough compared to the smallest acoustical wavelength of sound components of interest. Lai and Soedel discussed the transfer functions of two-dimensional thin shell and plate mufflers in detail, in which the point sound source model was developed to formulate acoustic equations and transfer functions of gas cavities [1,4]. Kim and Soedel developed a method to obtain the transfer matrix of three-dimensional cavities [5,6]. Zhou and Kim studied the singularity of the point source model at the source point and proposed a surface source model for solving the transfer matrix of three-dimensional acoustic systems [7].

*Corresponding author. Tel.: +86 21 34206664 323.
E-mail addresses: hzylzy@sjtu.edu.cn (Z. Huang), wkjiang@sjtu.edu.cn (W. Jiang).

0022-460X/$ - see front matter © 2007 Elsevier Ltd. All rights reserved.
doi:10.1016/j.jsv.2007.05.018

However, the acoustic pressure distribution on the source surface varies in a wide range so that two short pipes are added to the acoustic system and the boundary element method has to be utilized. Besides, CFD theories and experimental ways are also developed to get transfer matrices [8], which may be more time-consuming.

Here the point source model and surface source model for thin cavities are analyzed in brief, and then the circular line source model is developed based on the two-dimensional rectangular thin cavity. The computational results show that the singularity of source is canceled, uniform pressure distribution on the source is obtained and practicality in engineering problems is validated through the comparison between the circular line and circular surface source models.

2. Analysis of existing source models

A two-dimensional muffler element with rectangular thin panel volume is shown in Fig. 1. It has many engineering applications due to its convenient utilization.

2.1. Point source model

The acoustic wave equation of the cavity can be expressed as below [4]:

$$\frac{\partial^2 p}{\partial x^2}+\frac{\partial^2 p}{\partial y^2}-\left(\frac{1}{c^2}\right)\frac{\partial^2 p}{\partial t^2}=-\left(\frac{\ddot{m}}{h}\right)\delta(x-x^*)\delta(y-y^*), \tag{1}$$

where p is the acoustic pressure, $\ddot{m}$ defines the mass flow source, (x^*,y^*) is the coordinate of the source point, and $\delta(\cdot)$ indicates the Dirac delta function. In the frequency domain, the functions which define the four-pole parameter are:

$$f_i(x,y,\omega)=\sum_{m=0}^{\infty}\sum_{n=0}^{\infty}\frac{\mathrm{j}\omega\rho Q c^2 p_{mn}(x_i,y_i)p_{mn}(x,y)}{hN_{mn}[(\omega_{mn}^2-\omega^2)+2\mathrm{j}\omega\omega_{mn}\zeta_{mn}]}, \tag{2}$$

where

$$N_{mn}=\begin{cases} L_xL_y/4, & m,n=1,2,\ldots,\\ L_xL_y/2, & m=0,n=1,2,\ldots,\\ L_xL_y, & m=n=0. \end{cases} \tag{3}$$

Here $f_i(\cdot)$ means the pressure response at the observation point from the source point (x_i,y_i), ω represents the circular frequency, h is the thickness of the thin cavity, ρ is the average density of the gas in the cavity, c is the sound velocity, Q is the volume flow harmonic amplitude, ω_{mn} and $p_{mn}(x,y)$ are the natural frequencies and the natural modes of the cavity. L_x and L_y are the length and width of the cavity. Generally, the relationship

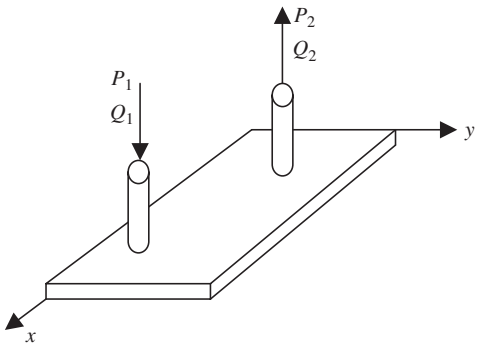

Fig. 1. The sketch of a rectangular thin plate type muffler.

between the input and output variables are:

$$\begin{bmatrix} Q_1 \\ P_1 \end{bmatrix} = \begin{bmatrix} A & B \\ C & D \end{bmatrix} \begin{bmatrix} Q_2 \\ P_2 \end{bmatrix}, \tag{4}$$

where P is the pressure response in the frequency domain and the parameters A, B, C, D are the transfer matrix parameters shown as below [4]:

$$A = \frac{f_2(x_2, y_2, \omega)}{f_1(x_2, y_2, \omega)}, \tag{5}$$

$$B = \frac{1}{f_1(x_2, y_2, \omega)}, \tag{6}$$

$$C = -f_2(x_1, y_1, \omega) + \left[f_1(x_1, y_1, \omega)/f_1(x_2, y_2, \omega)\right] f_2(x_2, y_2, \omega), \tag{7}$$

$$D = \frac{f_1(x_1, y_1, \omega)}{f_1(x_2, y_2, \omega)}. \tag{8}$$

The transfer matrix parameters can be obtained from Eqs. (2)–(8). However, parameters A, C and D include this term: $f_i(x_i,y_i,\omega)$, whose physical meaning is the pressure response at the source point (x_i,y_i), $i = 1,2$. Fig. 2 shows the pressure response at the source point (0.08, 0.07 m) as a function of the mode number at 2000 Hz, where $Q = 1$, $\rho = 6.04\,\mathrm{kg/m^3}$, $c = 162.9\,\mathrm{m/s}$, $L_x = 0.1\,\mathrm{m}$, $L_y = 0.1\,\mathrm{m}$, $h = 0.01\,\mathrm{m}$, $\zeta_{mn} = 0$.

The convergence rate of the solution is not convergent as depicted in Fig. 2. Obviously, some calculation errors will be encountered due to the singularity of the point source.

2.2. Surface source model

As shown in Ref. [8], the unit source strength is uniformly distributed on the source surface, which is assumed to be square for convenience. The source of unit strength is expressed as

$$\begin{aligned} \gamma &= \int\int_S -\left(\frac{\rho Q}{hL_xL_y}\right)\delta(x - x^*)\delta(y - y^*)\,\mathrm{d}s \\ &= \frac{\rho Q}{hL_xL_y}\left[H\left(x - x^* + \frac{l}{2}\right) - H\left(x - x^* - \frac{l}{2}\right)\right]\left[H\left(y - y^* + \frac{l}{2}\right) - H\left(y - y^* - \frac{l}{2}\right)\right], \end{aligned} \tag{9}$$

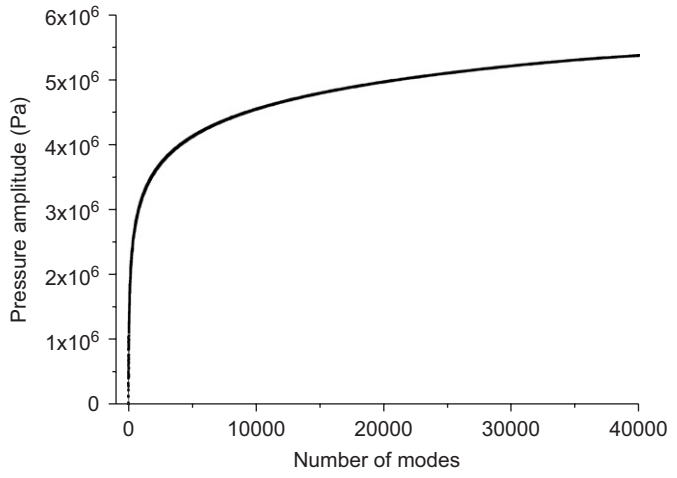

Fig. 2. Pressure response at the point source (2000 Hz).

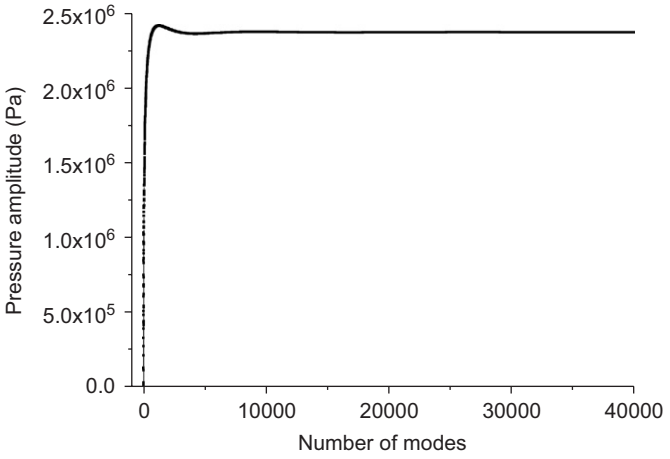

Fig. 3. Pressure response at the center of source surface (2000 Hz).

where $H(\cdot)$ is the unit step function, l is the length of square source surface, (x^*, y^*) is the coordinate of the center of the source surface. Hence, the pressure response on the center of the surface can be written as

$$P(x,y,\omega) = \mathrm{j}\rho c^2 \omega Q \sum_{m=0}^{\infty}\sum_{n=0}^{\infty} \frac{p_{mn}(x,y)B_x B_y}{hL_x L_y N_{mn}\left[(\omega_{mn}^2 - \omega^2) + 2\mathrm{j}\omega\omega_{mn}\zeta_{mn}\right]}, \tag{10}$$

where

$$B_x = \begin{cases} \dfrac{2L_x}{m\pi}\sin\left(\dfrac{m\pi l}{2L_x}\right)\cos\left(\dfrac{m\pi x^*}{L_x}\right), & m \neq 0, \\ l, & m = 0, \end{cases} \tag{11}$$

$$B_x = \begin{cases} \dfrac{2L_y}{m\pi}\sin\left(\dfrac{m\pi l}{2L_y}\right)\cos\left(\dfrac{m\pi x^*}{L_y}\right), & n \neq 0, \\ l, & n = 0. \end{cases} \tag{12}$$

The good convergence trend of pressure response is shown in Fig. 3. However, the computational formula of parameters A, C and D need to be averaged in this model. Also pressure distribution on the surface source is shown in Fig. 4, which gives so different pressure responses at different positions on the source surface. Hence, the averaging process of coefficient A, C and D is questionable due to the great variety on the surface. Accordingly, the circular line source model, a more convenient and new source model, is proposed to avoid this problem.

3. Circular line source model

3.1. Theoretical analysis

The pressure response of a point source in a thin acoustic cavity can be expressed as the combination of the direct response and the reflection of the boundary [8]

$$P(\vec{r},\omega) = \frac{\mathrm{j}\rho\omega Q}{4\pi|\vec{r} - \vec{r}^*|}\mathrm{e}^{-\mathrm{j}k|\vec{r} - \vec{r}^*|} + p_r(\vec{r},\omega), \tag{13}$$

where $\vec{r}$ and $\vec{r}^*$ are the locations of observation points and source points, $p_r(\vec{r},\omega)$ expresses the reflected waves from the boundaries.

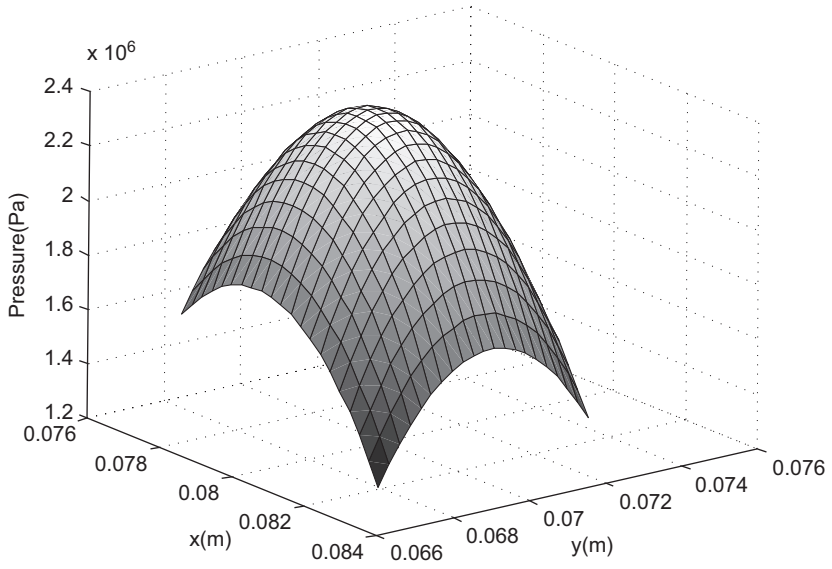

Fig. 4. Pressure distribution on the surface source (2000 Hz).

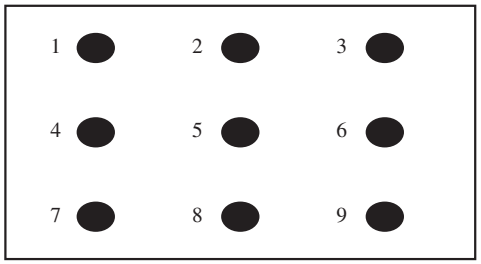

Fig. 5. The surface source composed of 9 discrete point sources.

As the distance of two points $|\vec{r}-\vec{r}^{*}|$ approaches 0, $P(\vec{r},\omega)$ becomes infinite. Surface source and circular line source are always finite due to the distributed strength of flow rate source. The wide range variation of pressure responses on the surface source is explained below. Surface source or circular line source can be regarded as the combination of infinite number of point sources, hence, Eq. (13) becomes:

$$P(\vec{r},\omega)=\sum\frac{\mathrm{j}\rho\omega Q}{4\pi|\vec{r}-\vec{r}^{*}|}\mathrm{e}^{-\mathrm{j}k|\vec{r}-\vec{r}^{*}|}+p_r(\vec{r},\omega). \tag{14}$$

For surface source, different total reciprocal value of $|\vec{r}-\vec{r}^{*}|$ of each point source contributes to different pressure responses on the surface. For example, the surface source is composed of nine point sources as shown in Fig. 5.

The distance between two points on the boundary is assumed to be 1. Respectively take point 1 and 5 as the observation point, then $\sum(1/|\vec{r}-\vec{r}^{*}|)=3+(2/\sqrt{5})+(3/2\sqrt{2})$ for observation point 1, and $\sum(1/|\vec{r}-\vec{r}^{*}|)=4+2\sqrt{2}$ for point 5. Hence the difference of pressure responses is explained through this example.

To avoid this problem, the circular source model is introduced as depicted in Fig. 6.Since the geometrical shape of input and output are circular in most engineering problems, the source strengths are concentrated on the circular line. The circular line source model is regarded as a source composed of infinite number of point sources and each point substitutes for a tiny sector. The pressure response at any position of the circular line keeps same due to its symmetry.

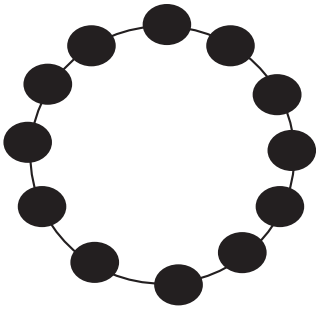

Fig. 6. The circular line source model composed of a large number of point sources.

The source of unit strength is written as

$$\gamma = \int_{L_s} -\left(\frac{\rho Q}{2\pi R_0 h}\right)\delta(\vec{r} - \vec{r}^*)\,\mathrm{d}s, \tag{15}$$

where R_0 is radius of the circular line. The pressure response in the thin cavity from the circular source is

$$P(x,y,\omega) = \mathrm{j}\rho c^2 \omega Q \sum_{m=0}^{\infty}\sum_{n=0}^{\infty} \frac{p_{mn}(x,y)}{2\pi R_0 h N_{mn}[(\omega_{mn}^2 - \omega^2) + 2\mathrm{j}\omega\omega_{mn}\zeta_{mn}]} \times \int_0^{2\pi} \cos\left(\frac{m\pi x^*}{L_x}\right)\cos\left(\frac{n\pi y^*}{L_y}\right) R_0\,\mathrm{d}\theta. \tag{16}$$

Finally, it can be written as

$$P(x,y,\omega) = \mathrm{j}\rho c^2 \omega Q \sum_{m=0}^{\infty}\sum_{n=0}^{\infty} \frac{p_{mn}(x,y)}{2\pi R_0 h N_{mn}[(\omega_{mn}^2 - \omega^2) + 2\mathrm{j}\omega\omega_{mn}\zeta_{mn}]} \times \int_0^{2\pi} \cos\left(\frac{m\pi(x_0 + R_0\cos\theta)}{L_x}\right)\cos\left(\frac{n\pi(y_0 + R_0\sin\theta)}{L_y}\right) R_0\,\mathrm{d}\theta, \tag{17}$$

where x_0 and y_0 represent the coordinates of the center of the circular line source. Although formula (16) and (17) are analytical solutions of the acoustic system, their integrals are difficult to obtain. In this work, the Newton–Cotes formula with fifth-order accuracy is utilized for improving solutions. If the circular line is divided into n parts, the error is

$$E_c = -\frac{2\pi}{1\,935\,360}\left(\frac{2\pi}{n}\right) f^{(6)}(\eta), \tag{18}$$

3.2. Numerical analysis

According to the computational parameters above, the good convergence trend of circular line source model is depicted in Fig. 7 together with other two source models.

According to the Fig. 7, the pressure response at the circular line source is convergent. Hence, more attention is paid to the distributed pressure responses on the circular line. The effects of source locations and sound frequency on the pressure response are analyzed as shown in Fig. 8. For convenience, the pressure ratio λ is defined as:

$$\lambda = \frac{P - P_0}{P_0}, \tag{19}$$

where P expresses the pressure response at any location, P_0 is the averaged pressure on the source.

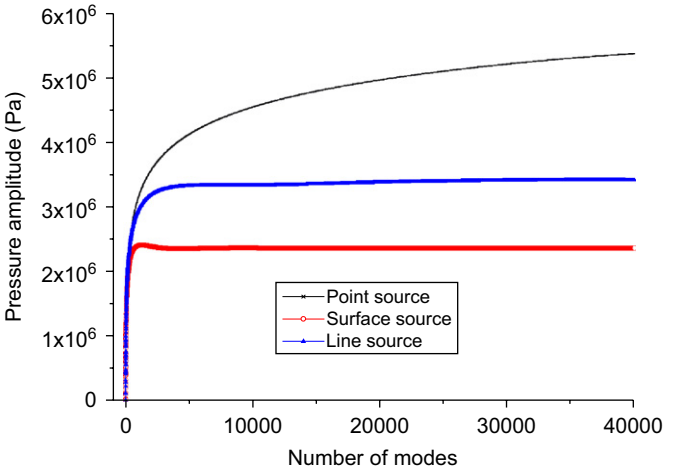

Fig. 7. Pressure response at one point of the line source (2000 Hz).

The pressure ratio curve as a function of circular angle at 2000 Hz is shown in Fig. 8(a), where the circular center is located at coordinate (0.05,0.05 m). Obviously, the pressure response on the circular source is uniform and the maximal error is only 0.07%.

While coordinate (0.08,0.07 m) is the circular line center, the pressure ratio as a function of the circular angle is depicted in Fig. 8(b)–(d), showing the relatively uniform pressure responses on the circular line source and tiny variety with various frequencies. When the center of the circular line moves to a new coordinate (0.09,0.09 m), which is the corner of the rectangular thin plate, the pressure ratio curve is shown in Fig. 8(e) and (f), where the maximal pressure ratio is less than 3%.

The pressure responses for 4 different length–width ratios of the rectangular plate are given in Fig. 9, where the circular center is placed at point (0.07,0.03 m). It is obvious that the pressure distribution on the circular line source is slightly relevant to the length–width ratio, which is caused by the second term of Eq. (13). The maximal pressure ratio is still less than 5%, which is applicable in engineering problems. It may be explained like this: "Since the difference of different positions is mainly coming from the first term in Eq. (14), the source line is very similar in its pressure magnitude."

From the discussion above, the circular line source model may be a good choice to calculate the transfer matrix of a two-dimensional acoustic system.

3.3. Practicality analysis

Since the actual source model is generally a circular surface, the comparison of averaged responses between the circular surface source model and the circular line source model is necessary. The sketch of the circular surface is depicted in Fig. 10.

The source of unit strength can be written as

$$\gamma = \int_{A_s} -\left(\frac{\rho Q}{\pi R^2 h}\right)\delta(\vec{r} - \vec{r}^{\,*})\,\mathrm{d}\sigma, \tag{20}$$

where R is radius of the circular surface and A_s is the area of the source surface. The pressure response in the thin cavity from the surface source is:

$$P(x,y,\omega) = \mathrm{j}\rho c^2 \omega Q \sum_{m=0}^{\infty}\sum_{n=0}^{\infty} \frac{p_{mn}(x,y)}{\pi R^2 h N_{mn}[(\omega_{mn}^2 - \omega^2) + 2\mathrm{j}\omega\omega_{mn}\zeta_{mn}]} \times \int_0^{2\pi}\int_0^{R} \cos\left(\frac{m\pi(x_0 + r\cos\theta)}{L_x}\right)\cos\left(\frac{n\pi(y_0 + r\sin\theta)}{L_y}\right) r\,\mathrm{d}r\,\mathrm{d}\theta, \tag{21}$$

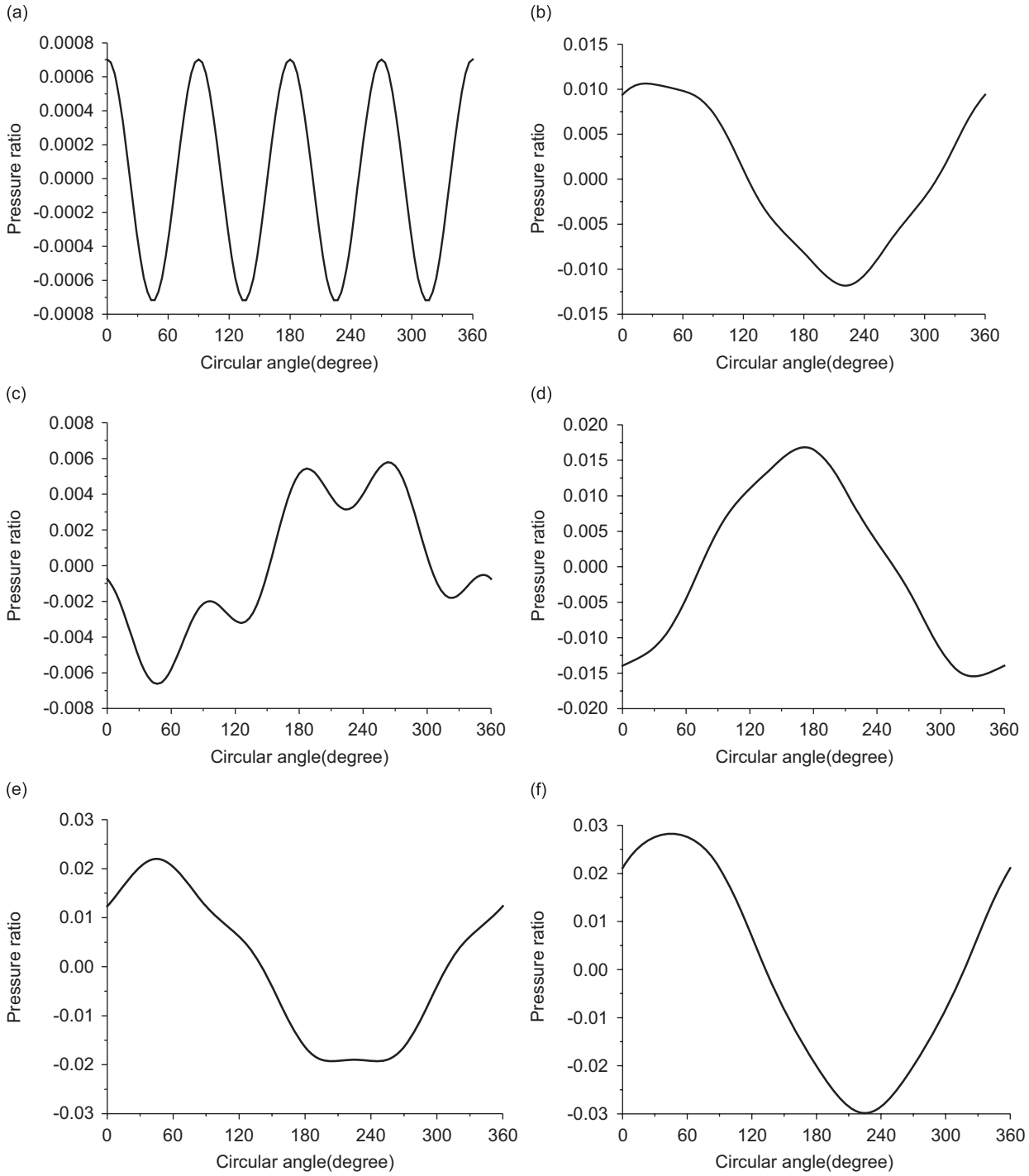

Fig. 8. Pressure ratio curve with circular angle at different conditions.

where x_0 and y_0 represent the coordinates of the center of the circular line source. Similar to the circular line source model, the numerical integration method is utilized to obtain solutions of the expression (21), which is very time-consuming compared to the computation of the line source model. The averaged response on the circular line model and actual surface model should be compared. The reasonable selection of circular radius

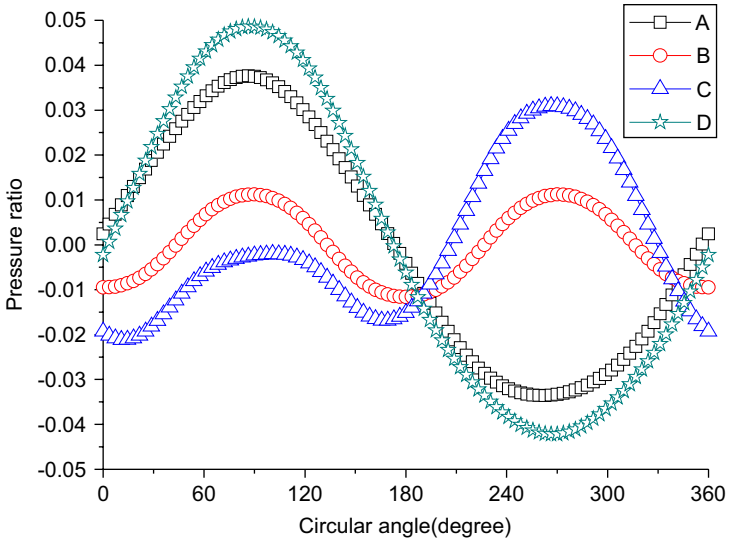

Fig. 9. Pressure ratio of different length width ratios (2000 Hz); squares: ratio = 0.1:0.08; circles: ratio = 0.1:0.06; triangles: ratio = 0.1:0.05; stars: ratio = 0.1:0.04; center coordinate: (0.07,0.03).

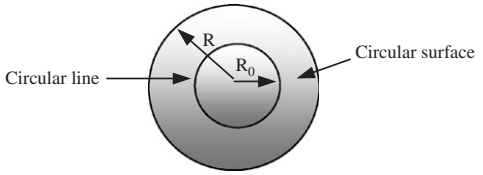

Fig. 10. The sketch of circular surface source model.

may be obtained from the following expression:

$$\frac{1}{A_s}\int_{A_s} P(x,y,\omega)\,\mathrm{d}\sigma = \frac{1}{L_s}\int_{S} P'(x,y,\omega)\,\mathrm{d}s. \tag{22}$$

The left term in this expression represents the averaged response on the circular surface source and the right term means the averaged pressure value on the circular line source. $P(x,y,\omega)$ and $P'(x,y,\omega)$ represents the response value on the surface source and the circular line source, respectively. A_s is the area of the surface source and L_s is the perimeter length of the circular line. Therefore, the combination of expressions (17), (21) and (22) may produce the following expression:

$$\begin{aligned}&\frac{1}{A_s}\int_{\sigma}\sum_{m=0}^{\infty}\sum_{n=0}^{\infty}\frac{p_{mn}(x,y)}{RN_{mn}[(\omega_{mn}^2-\omega^2)]}\int_0^{2\pi}\int_0^{R}\cos\left(\frac{m\pi(x_0+r\cos\theta)}{L_x}\right)\cos\left(\frac{n\pi(y_0+r\sin\theta)}{L_y}\right)r\,\mathrm{d}r\,\mathrm{d}\theta\,\mathrm{d}\sigma\\ &=\frac{1}{L_s}\int_{S}\sum_{m=0}^{\infty}\sum_{n=0}^{\infty}\frac{p_{mn}(x,y)}{2N_{mn}[(\omega_{mn}^2-\omega^2)]}\int_0^{2\pi}\cos\left(\frac{m\pi(x_0+R_0\cos\theta)}{L_x}\right)\cos\left(\frac{n\pi(y_0+R_0\sin\theta)}{L_y}\right)R_0\,\mathrm{d}\theta\,\mathrm{d}s.\end{aligned} \tag{23}$$

It is seen that the reasonable radius of the circular line may be obtained from the formula (23). However, since the expression is somewhat complicated, relationships between these parameters are not very clear. Therefore, the numerical calculations need to be employed to obtain the reasonable value of the circular line radius. The center location of sources is (0.08, 0.07 m) and the pressure responses on the line source as a function of the circular source radius are depicted in Fig. 11, where the averaged responses on the circular surface source are also displayed at some typical frequencies, such as, 400, 800, 1000, 1200, 1400 and 2000 Hz.

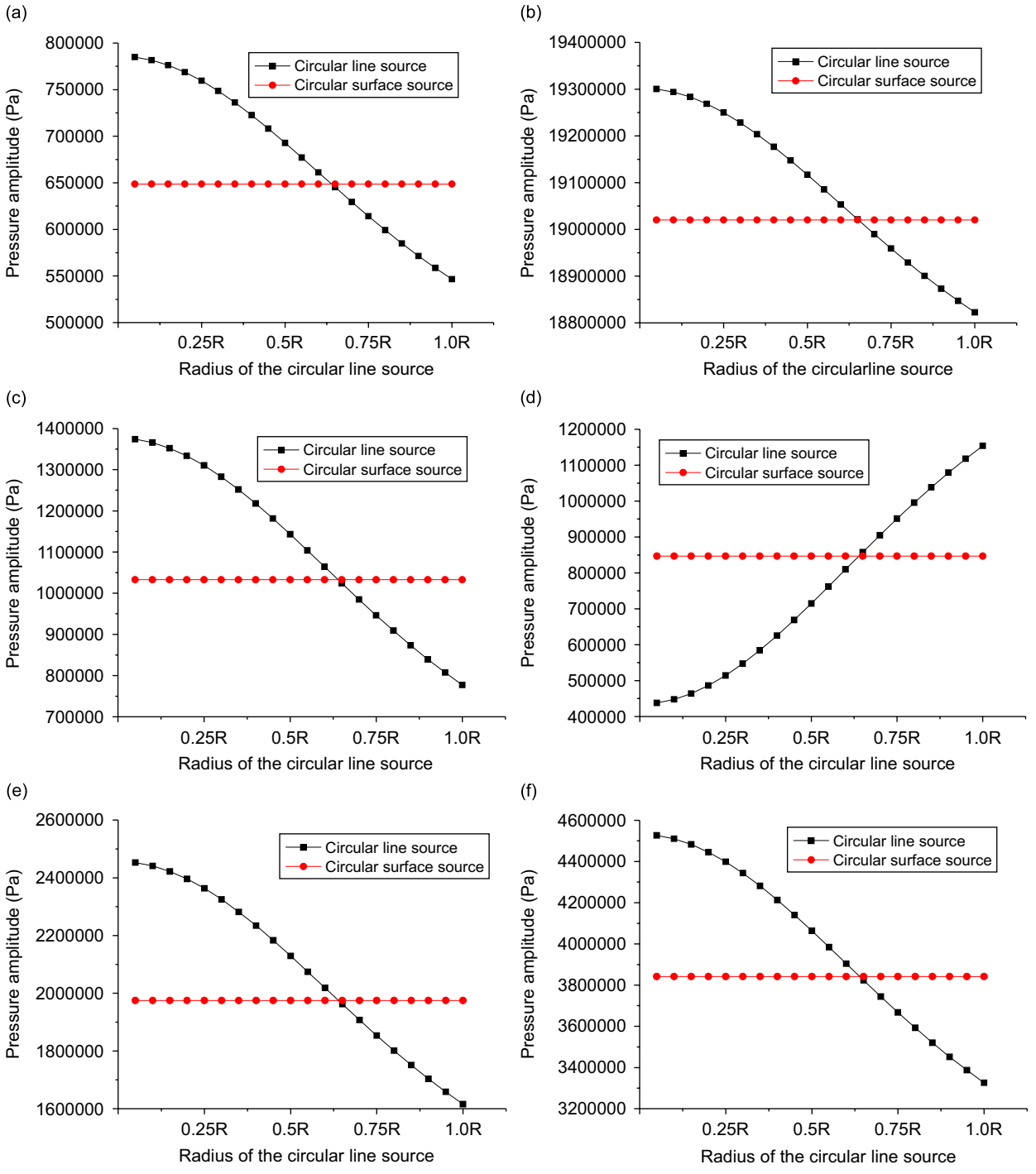

Fig. 11. Comparison of pressure responses between two models: (a) 400; (b) 800; (c) 1000; (d) 1200; (e) 1400; (f) 2000 Hz.

It can be seen from Fig. 11 that the pressure amplitudes of two models are very close at such typical frequencies as 400, 1000, 1200, 1400 and 2000 Hz when the radius of circular line source is limited in 0.63~0.65 R. Not all the figures are depicted in this section due to the paper length limit. Compared to the wavelength of sound components of interest, the dimension of the sources is very small. Thereby, the pressure responses on the sources are not greatly affected by the tiny change of the source dimension, which has been

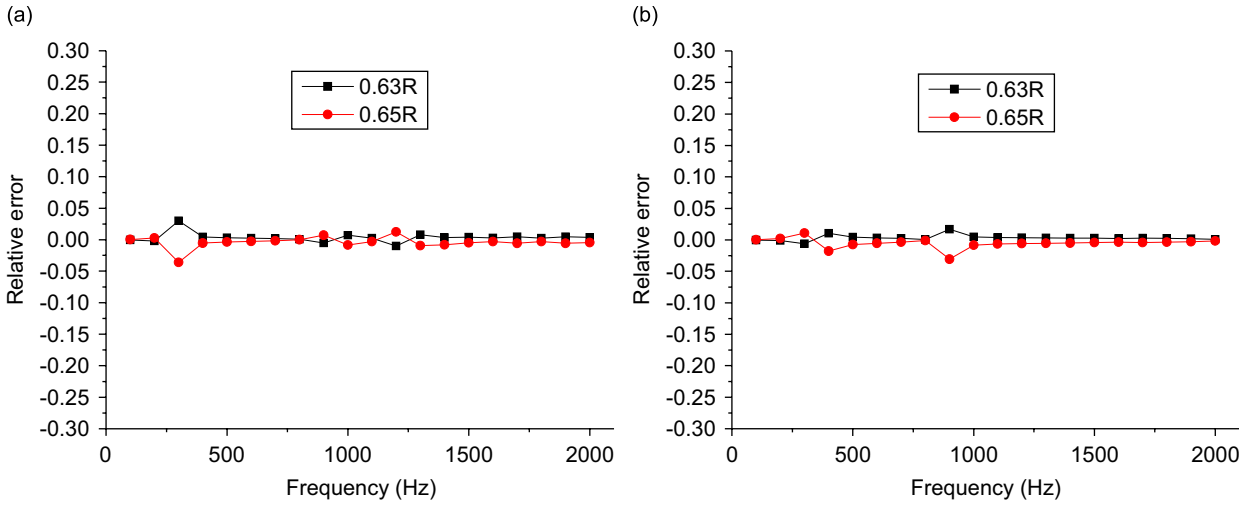

Fig. 12. The relative error between the two source models at the radius of 0.63R and 0.65R: (a) source location: (0.08,0.07), length–width ratio: 0.1:0.1; (b) source location: (0.07, 0.04), length–width ratio: 0.1:0.08.

displayed in Fig. 11(b). Since the frequency 800 Hz is very close to the first-order resonance frequency 814 Hz, the pressure responses at the frequency are very large and vary few with the variety of radius so that the radius value in a very wide range could be selected. The relative errors of the two models are defined as

$$\mathrm{Err} = \frac{\bar{P}_{\text{line source}} - \bar{P}_{\text{surface source}}}{\bar{P}_{\text{surface source}}}. \tag{24}$$

The relative errors from 100 to 2000 Hz are depicted in Fig. 12(a). Also the effects of cavity dimension and source locations on the averaged pressure responses are investigated. Fig. 12(b) depicts the relative errors at a different condition that the location of source center is (0.07,0.04) and the length–width ratio is 0.1:0.08.

It can be seen from Fig. 12 that the relative errors between the two models are very small. Moreover, since the source dimension is greatly less than the wavelength of the acoustic component of our interest and the cavity dimension, the relative error is not obviously affected by the change of source locations and cavity length–width ratio. These errors may be caused by the approximate line source model and computational accuracy. The circular line source model has many superiorities to the circular surface source model, such as simple model, convenient computation and uniform responses on the source. Therefore, this model could be utilized in engineering problems.

4. Conclusions

The source models for calculating the transfer matrix of two-dimensional thin acoustic cavities are investigated in detail. Based on theoretical analysis and computational examples, some conclusions can be obtained:

(1) The divergence of the point source can be avoided by the utilization of the surface source model. However, the pressure distribution on the source surface varies a very wide range, which might make trouble in the averaging procedure. Especially for the actual circular surface source, the computation about transfer matrix coefficients is very time-consuming.
(2) The proposed circular line source model can be considered a reasonable one in engineering. The convergence characteristic can be improved in comparison to the point source model and the pressure responses on the circular source are relatively uniform compared to the surface source model. Even if the

length–width ratio is relatively large, the circular source model is valid. The new model can be easily used to formulate four pole matrices of two-dimensional acoustic systems.

(3) Given a reasonable value of the circular radius, the averaged values on the circular line source are very close to that on the circular surface source, which validates the practicality of the circular line source.

References

[1] P.C.-C. Lai, W. Soedel, Two-dimensional analysis of thin shell or plate-like muffler elements of non-uniform thickness, *Journal of Sound and Vibration* 195 (1996) 445–475.

[2] J.P. Elson, W. Soedel, Simulation of the interaction of compressor valves with acoustic back pressure in long discharge lines, *Journal of Sound and Vibration* 34 (1974) 211–220.

[3] P.C.-C. Lai, W. Soedel, Gas pulsations in thin, curved or flat cavities due to multiple mass flow sources with special attention to multi-cylinder compressor, *Journal of Sound and Vibration* 197 (1996) 45–66.

[4] P.C.-C. Lai, W. Soedel, Two-dimensional analysis of thin shell or plate-like muffler elements, *Journal of Sound and Vibration* 194 (1996) 137–171.

[5] J. Kim, W. Soedel, General formulation of four pole parameters for three-dimensional cavities utilizing modal expansion, with special attention to the annular cylinder, *Journal of Sound and Vibration* 129 (1989) 237–254.

[6] J. Kim, W. Soedel, Analysis of gas pulsations in multiply connected three-dimensional acoustic cavities with special attention to natural mode or wave cancellation effects, *Journal of Sound and Vibration* 131 (1989) 103–114.

[7] W. Zhou, J. Kim, Formulation of four poles of three-dimensional acoustic systems from pressure response functions with special attention to source modeling, *Journal of Sound and Vibration* 219 (1999) 89–103.

[8] P. Cyklis, Experimental identification of the transmittance matrix for any element of the pulsating gas manifold, *Journal of Sound and Vibration* 244 (2001) 859–870.